phys. stat. sol. (b) **231**, No. 1, 213–221 (2002)

Bragg Diffraction of X-Rays by Single Crystals with Large Microdefects III. High-Resolution Diffraction Measurements[1])

E. N. Kislovskii[2]) (a), S. I. Olikhovskii (a), V. B. Molodkin (a), V. V. Nemoshkalenko (a), V. P. Krivitsky (a), E. G. Len (a), E. V. Pervak (a), G. E. Ice (b), and B. C. Larson (b)

(a) Institute for Metal Physics, National Academy of Sciences of Ukraine, Vernadsky blvd. 36, 03680 Kyiv 142, Ukraine

(b) Oak Ridge National Laboratory, Oak Ridge, TN 37831-6118, USA

(Received July 17, 2000; in revised form December 17, 2001; accepted December 19, 2001)

Subject classification: 61.10.Dp; 61.72.Bb; S5.11

The generalized dynamical theory of X-ray scattering by single crystals containing randomly distributed microdefects has been applied to characterize structural imperfections in the Czochralski-grown dislocation-free silicon sample annealed at 1080 °C during 6 h. Measurements of rocking curves for 111 and 333 reflections of $CuK_{\alpha 1}$ radiation have been performed by the high-resolution double-crystal diffractometer. The sizes and concentrations of oxygen precipitates and dislocation loops, which have been determined by independent fitting of the two rocking curves, are in good agreement confirming the validity of the developed theory.

Обобщенная динамическая теория рассеяния рентгеновских лучей монокристаллами, содержащими случайно распределенные микродефекты, применена для диагностики структурных несовершенств в образце бездислокационного кремния, выращенного методом Чохральского и отожженного при 1080 °C в течение 6 ч. Измерения кривых качания для отражений 111 и 333 излучения $CuK_{\alpha 1}$ были выполнены на высокоразрешающем двухкристальном дифрактометре. Размеры и концентрации преципитатов кислорода и дислокационных петель, которые были определены путем независимой подгонки двух кривых качания, находятся в хорошем взаимном согласии, подтверждающем правильность разработанной теории.

1. Introduction

The measurement of diffuse scattering (DS) intensity distributions in the reciprocal lattice space can provide the most complete diffractometric information about structural defects in crystals [1]. In practice, however, any X-ray diffractometer has a finite resolution and, consequently, the scattered X-ray intensity is integrated partially, which leads to some loss of obtainable information. On the other hand, the increasing resolution causes a reduction in gained diffraction intensity. Therefore, X-ray diffractometric measurements by double-crystal diffractometry (DCD) are still extensively used representing a compromise between the volume of obtained information and sensitivity of measurements.

Particularly, the method of integral DS, that has been proposed by Dederichs [2, 3] and developed by Larson [4, 5], is widely applied to characterize point defects and their

[1]) Parts I and II, see phys. stat. sol. (b) **227**, 429 (2001) and **231**, 199 (2002).
[2]) Corresponding author; e-mail: ekis@imp.kiev.ua

© WILEY-VCH Verlag Berlin GmbH, 13086 Berlin, 2002 0370-1972/02/23105-0213 $ 17.50+.50/0

clusters in various crystalline materials [6–14]. In this method, the angular dependencies of DS intensity integrated over exit angles, which are measured by DCD with a wide open detector window, are treated using the formulas derived for various types of defects from the known expressions of the kinematical theory for the differential DS intensity [1, 2, 15, 16]. The method is very effective due to the high sensitivity of these dependencies to defect sizes and concentrations.

However, in the investigations of microdefects in silicon single crystals [17–19], this method encounters difficulties. Firstly, the measurable DS intensity distributions are very close to the Bragg peak because of the large effective sizes of microdefects. In such cases, at sufficiently high microdefect concentrations giving DS intensity comparable with coherent component, the correct interpretation of the measured angular distributions of X-ray scattering intensity in this region requires taking into account the dynamical DS effects and the contribution of the coherent component. Secondly, it is necessary to account for the simultaneous presence of several types of microdefects in the silicon crystal, namely, oxygen precipitates, dislocation loops, stacking faults etc. [20, 21].

These difficulties can be overcome using the generalized dynamical theory of X-ray scattering by single crystals that contain homogeneously distributed defects [22–26]. This theory has been extended in Refs. [27, 28] to the case of single crystals with microdefects having large effective radii comparable with the extinction length. Here, the analytical expressions derived in Refs. [27, 28] for the coherent and diffuse components of reflection power of such crystals, which have been integrated over exit angles, will be applied to characterize microdefects in an annealed silicon single crystal using rocking curves measured by high-resolution DCD with a wide open detector window.

X-ray optic schemes of the measurements and the investigated silicon sample are described in Section 2. The measurement of rocking curves is explained and the obtained results are discussed in Section 3. The formulas from Ref. [27] and Ref. [28] will be referred to as (I.1) etc. and (II.1) etc., respectively.

2. Experimental Setup and Investigated Sample

The measurements of rocking curves of the investigated silicon sample, which was in the parallel non-dispersive setting relatively to the last reflection of the collimator, were performed using a high-resolution four-circle X-ray DCD (Fig. 1). In the case of symmetric 111 reflections at the sample, the collimator consisted of two separated three-reflection channel-cut perfect Si monochromators in the antiparallel (dispersive) setting with symmetric 220 reflections (Fig. 1a). For symmetric 333 reflections at the sample, the first one-reflection Ge monochromator and the second two-reflection channel-cut Si monochromator in the antiparallel setting were both used with symmetric 333 reflections (Fig. 1b). The $CuK_{\alpha 1}$ radiation was emitted by a 1.2 kW ($V = 30$ kV, $I = 40$ mA) X-ray tube with minimum projection of the focus $0.4 \times 8\ \mathrm{mm}^2$. In the optical schemes used, the vertical divergence was estimated to be approximately 10 arc min, the horizontal divergences were less than 5 arcsec and 2 arcsec for 111 and 333 reflections, respectively. The irradiated sample surface area was $0.25 \times 2.0\ \mathrm{mm}^2$. The specimen was rotated around a vertical axis by a stepping motor controlled by a computer in steps of 0.4 arcsec and 0.2 arcsec for 111 and 333 reflections, respectively.

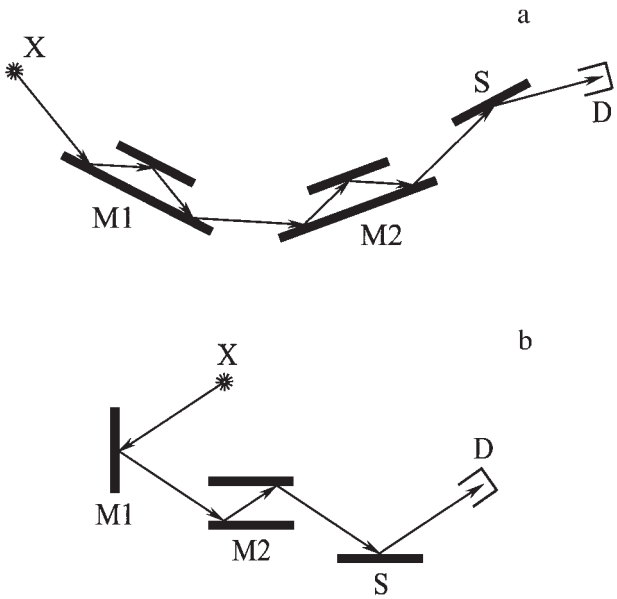

Fig. 1. High-resolution diffraction schemes for measurements of rocking curves for symmetric Bragg reflections Si 111 (a) and 333 (b) using CuK_{α_1} radiation. Notation: X X-ray tube, M1 and M2 monochromators, S sample, D detector

The investigated sample of a dislocation-free silicon single crystal with a thickness of 488 μm was cut perpendicularly to the growth axis [111] from a Czochralski-grown ingot with p-type conductivity ($\varrho = 10$ Ω cm) and with an oxygen concentration of 1.1×10^{18} cm^{-3} and a carbon concentration lower than 1×10^{16} cm^{-3}, respectively. The sample was annealed in the air at 1080 °C for 6 h.

In the transmission X-ray topograph of the annealed sample, which was obtained in symmetric Laue reflection of $MoK_{\alpha 1}$ radiation (Fig. 2), the homogeneous distribution of microdefects can be seen with contrast dimensions not exceeding 50 μm and the number density estimated to be not less than 1×10^5 cm^{-3}.

Fig. 2. Lang topograph of the annealed silicon sample (the symmetric 220 reflection of $MoK_{\alpha 1}$ radiation), ten-fold magnification

3. Treatment of Experimental Results and Discussion

It is well known (see, e.g., Refs. [20, 21]) that in the Czochralski-grown silicon, which is the supersaturated solid solution of oxygen, the oxygen precipitates grow during the annealing at elevated temperatures. The high stress at the interface between the silicon matrix and SiO_x particles ($x \approx 2$) is released by the emission of interstitial silicon atoms, which agglomerate into dislocation loops and stacking faults. There exist various theories, which give the analytical description of precipitation and growth kinetics of new phase particles in supersaturated solid solutions [29–35]. These theories, however, ignore (except for Ref. [32]) the presence of dislocation loops formed by interstitial atoms, which are emitted by new phase particles, and their influence on the precipitate growth kinetics. To describe in details the growth and dissolution kinetics of precipitates and loops, it is necessary, in general, to solve numerically the set of coupled second order differential discrete rate equations for small defect sizes and Fokker-Planck equations for larger ones [36]. The solutions of these equations give the distribution functions for size and density of the microdefects (precipitates and stacking faults) versus annealing time and temperature. Corresponding numerical calculations, however, are very time-consuming, even for modern computers, and cannot be while used as a routine tool.

On the other hand, both numerical and analytical approaches are based on model assumptions and contain some physical parameters to be refined. It is clear, that in order to check all these theories a method to diagnose structural parameters of such systems is necessary, which permits to receive information from statistically significant crystal volumes. Additionally, in case of supersaturated solid solution of oxygen in silicon, such method should allow to diagnose simultaneously parameters of different types of defects with arbitrary sizes. The existing methods for diagnostics of imperfections in silicon (transmission electron microscopy, method of infrared absorption, X-ray topography, optical microscopy of etch pits) have the exclusively important role for an establishment of a nature of imperfections, but have restrictions in reference to researched crystal volumes and defect sizes (see, e.g., Ref. [21]). The X-ray diffraction method of diagnostics using angular DS intensity distributions from imperfections is to a large extent free of such restrictions. The existing problem of diagnostics of large microdefects, DS intensity from which is concentrated under Bragg peak, has been solved in the previous publications [27, 28], where the self-consistent description of dynamical coherent and diffuse scattering in the total reflection range has been given and the explicit analytical expressions have been derived for the corresponding components of crystal reflectivity.

Here, we demonstrate the application of the generalized method of integral DS for the determination of microdefects characteristics in annealed silicon single crystal. This procedure is based on the analytical expressions for coherent and diffuse reflectivity components integrated over exit angles for single crystals with randomly distributed microdefects [27, 28].

The rocking curves for 111 and 333 reflections of $CuK_{\alpha 1}$ radiation, which have been measured in the symmetric Bragg diffraction geometry, are shown in Figs. 3 and 4, respectively. It is remarkable that due to the high-resolution optical schemes used one can observe the extinction gap in the diffuse component of reflectivity, which has been obtained by subtracting the fitted coherent component of reflectivity from the measured rocking curve. This gap is seen for both reflections (Figs. 3b and 4b) and, to our knowledge, has been demonstrated experimentally for the first time.

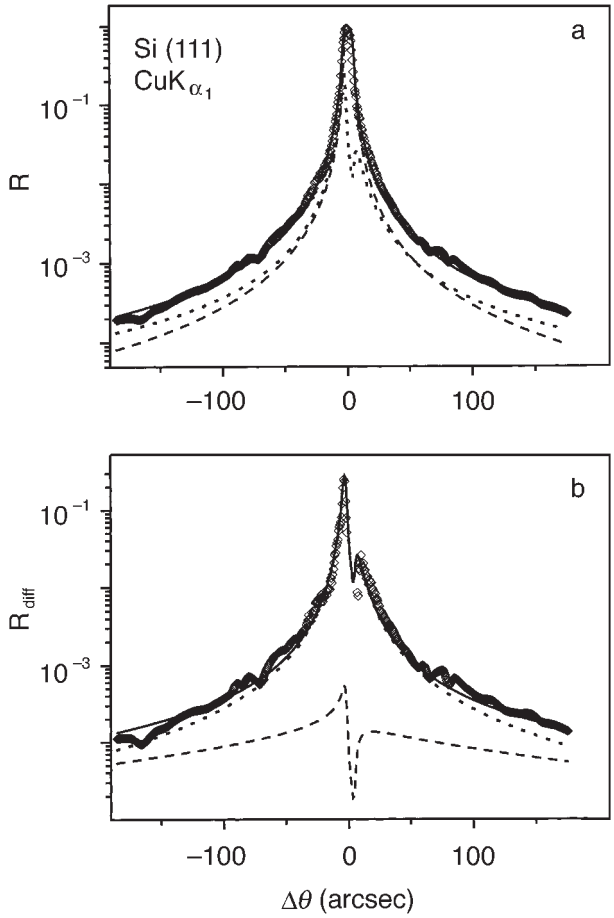

Fig. 3. a) Rocking curve of the silicon sample annealed for 6 h at 1080 °C for the symmetric Bragg reflection 111 of CuK$_\alpha$ radiation. The fitted total rocking curve, its coherent (R_{coh}) and diffuse (R_{diff}) components are plotted by solid, dashed, and dotted lines, respectively. b) The "extracted" experimental diffuse component has been obtained by subtracting calculated R_{coh} from the measured rocking curve, the theoretical diffuse component R_{diff} and its components resulting from dislocation loops and precipitates are plotted by solid, dotted, and dashed lines, respectively

In the fitting procedure, the defect radii and concentrations were the fit parameters. The high sensitivity of the rocking curves to the fit parameters has required also to refine the zeroth position of the $\Delta\theta$-scale. To obtain a more accurate fitting in the vicinity of and within the total reflection range, the intrinsic reflection coefficient of the investigated sample

$$R(\Delta\theta) = R_{coh}(\Delta\theta) + R_{diff}(\Delta\theta)\,,$$

where the coherent (R_{coh}) and diffuse (R_{diff}) components are defined by Eqs. (I.34) and (II.46), respectively, was convoluted with the reflection coefficient of the collimator system at the final stage of the fitting procedure.

To characterize the fit quality the weighted agreement factor was used:

$$R_W = \chi/f\,, \qquad \chi^2 = \sum_{j=1}^{M} w_j\left(R_j^{calc} - R_j^{meas}\right)^2,$$

$$f^2 = \sum_{j=1}^{M} w_j\left(R_j^{meas}\right)^2, \qquad w_j = \left(\sigma_j R_j^{meas}\right)^{-2},$$

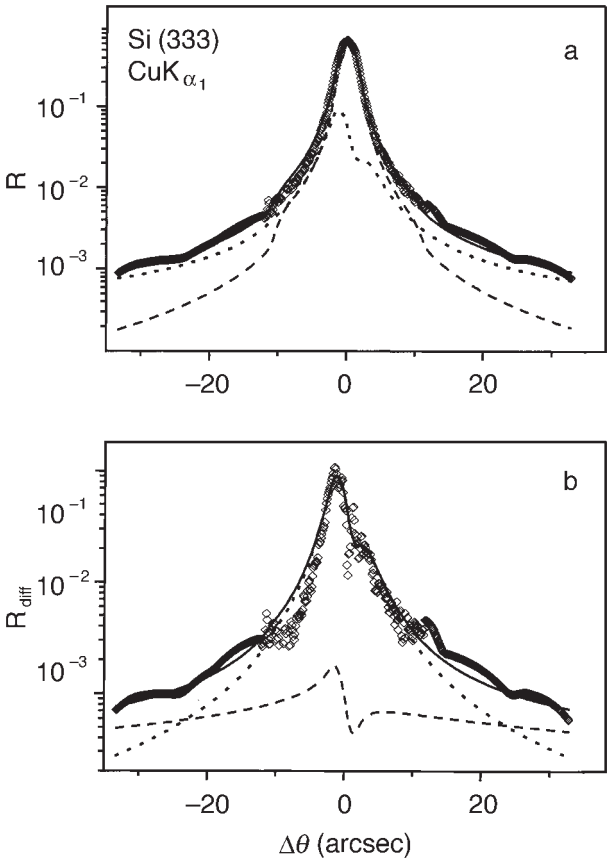

Fig. 4. See caption of Fig. 3, 333 reflection of CuK$_\alpha$ radiation

where R_j^{meas} and R_j^{calc} are the measured and calculated reflectivities at the angular positions $\Delta\theta_j$ of the sample, respectively, M is the number of measurement points, and σ_j^2 is the mean-square deviation of the j-th measured point. Such a R_w-factor is usually applied to give the uniform estimate of the fit quality for measured intensity dependencies within the whole measurement range (see, e.g., Ref. [37]). The obtained fitting results were characterized also by the agreement R-factor calculated with weight $w_j = \sigma_j^{-2}$. This factor describes the fit quality mainly in the total reflection range, where the peak intensity is observed.

In the first step of the treatment, we have restricted ourselves to the most simplified microdefect models supposing subsequently the presence (i.e., the dominant influence on the diffraction pattern) of only spherical clusters (precipitates) or circular dislocation loops. The spherical cluster model gave the unrealistic low number densities of precipitates about $n_P = c_P/V_c \approx 10^2$ cm^{-3} with the obtained large precipitate radii of about $R_P \approx 9$ µm and was recognized as unacceptable (c_P is the precipitate concentration per lattice site and V_c is the unit cell volume). For the dislocation loop model, supposing the random distribution of prismatic dislocation loops with Burgers vector $\mathbf{b} = \frac{1}{2}\langle 110\rangle$, the best fit values of the parameters that have been obtained are $R_L \approx 9$ µm, $n_L = c_L/V_c \approx 2 \times 10^6$ cm^{-3} for both reflections.

In a second step, we fitted the measured rocking curves taking into account the presence of both types of microdefects (loops and precipitates) simultaneously. The corresponding modification of the formulas obtained in Refs. [27, 28] can be made easily, if the random distribution of defects of both types is supposed to be without mutual correlation. Generally, the correlation between growing precipitates particles and dislocation loops emitted by them has been observed experimentally (see, e.g., [20, 21]). Also, the colonies of precipitates are encountered near dislocation loop lines. However, after sufficiently large annealing times the predominate part of microdefects of both types is chaotically distributed in the crystal volume. In such a case, the ensemble averaging can be performed independently for each defect type and results in replacing the parameters $L_{\mathbf{H}}$ and μ_{ds} in Eqs. (I.34) and (II.46) for R_{coh} and R_{diff}, respectively, with the corresponding sums of these parameters calculated for each type of defects:

$$L_{\mathbf{H}} = \sum_{\alpha} L_{\mathbf{H}}^{\alpha}\,, \qquad \mu_{\mathrm{ds}} = \sum_{\alpha} \mu_{\mathrm{ds}}^{\alpha}\,.$$

Here, α enumerates the defect types.

The exponent $L_{\mathbf{H}}$ of the static Debye-Waller factor for precipitates was calculated according to the known expression [16] modified for the case of disc-shaped clusters as follows:

$$L_{\mathbf{H}} \cong \begin{cases} c_{\mathrm{P}} n_0 \eta^2/2\,, & \eta^2 \ll 10 \\ c_{\mathrm{P}} n_0 \eta^{3/2}\,, & \eta^2 \gg 10\,, \end{cases}$$

where $n_0 = \pi R_{\mathrm{P}}^2 h_{\mathrm{P}}/V_{\mathrm{c}}$ is the number of unit cells substituted by precipitate volume, h_{P} is the precipitate thickness, $\eta = \alpha_0 n_0^{1/3} H a_0/(2\pi)$, $\alpha_0 = \Gamma\varepsilon(3\pi^2/4)^{1/3}$, H is the modulus of the reciprocal lattice vector, and a_0 is the lattice constant. The cluster power has been also modified for the clusters of the disc-shaped form as $A_{\mathrm{cl}} = \Gamma\varepsilon R_{\mathrm{P}}^2 h_{\mathrm{P}}/2$. In the fitting, the precipitate thickness was assumed to be equal $h_{\mathrm{P}} = 2R_{\mathrm{P}}/r_{\mathrm{a}}$, and the aspect ratio r_{a} was determined by solving numerically the transcendental equation, which connects the diameter of the disc-shaped precipitate with its radius R_{P}, and which has been obtained by minimizing the total free energy of the precipitate [34]. The parameter of the deformation at the amorphous SiO_2 precipitate boundary was set equal to $\varepsilon \approx 0.0242$ [38].

The values of microdefect characteristics determined by fitting the measured rocking curves for two types of microdefects simultaneously are listed in the Table. As can be seen, the sizes and densities of precipitates and dislocation loops, which have been determined independently for each reflection, are in a good mutual agreement. The densities and sizes of dislocation loops well correspond to the results of X-ray topographic observation (Fig. 2). It is clear, that precipitates with sizes of about 0.6 μm cannot be resolved with a X-ray topograph, but the obtained sizes and densities of precipitates, as well as those of dislocation loops, satisfactorily correlate with known results of direct observations [32, 39–43] and theoretical calculations [42, 43] for silicon single crystals with similar characteristics (initial concentration of oxygen and carbon, temperature and duration of an annealing). Namely, Patel [39] has observed on a X-ray topograph from a Si sample, annealed at 1000 °C for 6 h, dislocation loops with radii of about 10 μm, and for these loops by results of measurements of anomalous X-rays transmission has estimated their density to be about 10^6 cm^{-3}. The dimensions of etch pits from stacking faults in silicon annealed at 1105 °C for 5 h, which have been observed by Patel et al. [32] and Murarka [40] using an optical microscope, were 10 and 14 μm,

Table 1
Characteristics of oxygen precipitates and dislocation loops in silicon sample annealed at 1080°C for 6 h

hkl	111	333
n_P (cm^{-3})	5.8×10^9	5.4×10^9
R_P (μm)	0.66	0.57
h_P (Å)	135	127
n_L (cm^{-3})	5.9×10^5	4.2×10^5
R_L (μm)	16.6	16.0
R (%)	9.4	4.5
R_w (%)	10	18

respectively. Patrick et al. [41], using the transmission electron microscope, observed in silicon annealed at 1000 °C during 8 h the plate-like precipitates with sizes of about 0.16 μm and thickness of about 100 Å. In similar observations of Wada et al. [42], after annealing at 1050 °C for 6 h, the sizes of plate-like precipitates with thickness 40 Å were about 0.5 μm. The densities of precipitates after similar thermal treatment, as determined by Livingston et al. [43] using optical methods, was about 2×10^9 cm^{-3}. Altogether, all these values of the microdefect parameters, which have been obtained by various researchers using different investigation methods for silicon samples being analogous, to more or less extent, to that investigated by us, are sufficiently close related to the values of microdefect characteristics, which have been determined in the present investigation (see Table 1).

Thus, the good mutual agreement of the values of defect characteristics determined from the rocking curves for two reflections and the fair correlation of these parameters with the published experimental data can be considered as the experimental verification of the developed generalized method of integral DS as well as the demonstration of its high diagnostic possibilities. In order to bring off these possibilities, however, it is necessary to use the additional experimental and theoretical information about nature and morphology of defects in single crystals under investigation.

4. Summary

The generalized dynamical theory of X-ray scattering by imperfect single crystals was used to analyze the total rocking curves of silicon single crystals containing simultaneously large (dislocation loops and stacking faults) and small (oxygen precipitates) defects. The analytical expressions for coherent and diffuse components of crystal reflectivity integrated over exit angles form the theoretical foundation for the generalized method of integral DS, which has allowed to treat the measured rocking curves in the whole angle range including the total reflection range and to determine the microdefect characteristics with good precision and without any restrictions on the defect sizes.

Acknowledgements This research was supported by grant No. UP1-336 of the U.S. Civilian Research and Development Foundation, and project No. 02.07/00008 of the Fund of Fundamental Investigations of the Ministry for Education and Science of Ukraine.

References

[1] M. A. Krivoglaz, X-Ray and Neutron Diffraction in Nonideal Crystals, Springer-Verlag, Berlin/Heidelberg/New York/London/Paris/Tokyo 1993.
[2] P. H. Dederichs, Phys. Rev. B **4**, 1041 (1971).
[3] J. E. Thomas, T. O. Baldwin, and P. H. Dederichs, Phys. Rev. B **3**, 1167 (1971).
[4] B. C. Larson and F. W. Young, Jr., Z. Naturforsch. A **28**, 626 (1973).
[5] B. C. Larson, J. Appl. Crystallogr. **8**, 150 (1975).
[6] P. H. Dederichs, J. Phys. F **3**, 471 (1973).
[7] B. C. Larson and F. W. Young, Jr., phys. stat. sol. (a) **104**, 273 (1987).
[8] P. Ehrhart and R. S. Averback, Philos. Mag. A **60**, 283 (1989).
[9] K. Karsten and P. Ehrhart, Phys. Rev. B **51**, 10508 (1995).
[10] A. N. Morozov and V. T. Bublik, J. Cryst. Growth **97**, 475 (1989).
[11] L. A. Charniy, A. N. Morozov, V. T. Bublik, K. D. Scherbachev, I. V. Stepantsova, and V. M. Kaganer, J. Cryst. Growth **118**, 163 (1992).
[12] P. Franzosi, J. Cryst. Growth **126**, 85 (1993).
[13] R. J. Matyi, M. R. Melloch, K. Zhang, and D. L. Miller, J. Phys. D **28**, A139 (1995).
[14] T. Yamazaki and I. Hashimoto, Phys. Rev. B **56**, 5228 (1997).
[15] H. Trinkaus, phys. stat. sol. (b) **51**, 307 (1972).
[16] H. Trinkaus, phys. stat. sol. (b) **54**, 209 (1972).
[17] J. R. Patel, J. Appl. Crystallogr. **8**, 186 (1975).
[18] V. Holý and J. Kubena, phys. stat. sol. (b) **170**, 9 (1992).
[19] R. Bouchard, J. R. Schneider, S. Gupta, S. Messoloras, R. J. Stewart, H. Nagazawa, and W. Zulehner, J. Appl. Phys. **77**, 553 (1995).
[20] C. Claeys and J. Vanhellemont, J. Cryst. Growth **126**, 41 (1993).
[21] A. Borghesi, B. Pivac, A. Sassella, and A. Stella, J. Appl. Phys. **77**, 4169 (1995).
[22] V. B. Molodkin and E. A. Tikhonova, Fiz. Met. Metalloved. **24**, 385 (1967).
[23] V. B. Molodkin, Metallofizika **2**, 3 (1980) [Phys. Metals **3**, 573 (1981)]; Metallofizika **3**(4), 27 (1981) [Phys. Metals **3**, 615 (1981)].
[24] V. B. Molodkin, S. I. Olikhovskii, and M. E. Osinovskii, Metallofizika **5** (1), 3 (1983) [Phys. Metals **5**, 1 (1984)].
[25] A. N. Kostyuk, V. B. Molodkin, and S. I. Olikhovskii, phys. stat. sol. (b) **178**, 45 (1993).
[26] V. B. Molodkin, S. I. Olikhovskii, and A. N. Kostyuk, phys. stat. sol. (b) **183**, 59 (1994).
[27] V. B. Molodkin, S. I. Olikhovskii, E. N. Kislovskii, E. G. Len, and E. V. Pervak, phys. stat. sol. (b) **227**, 429 (2001).
[28] S. I. Olikhovskii, V. B. Molodkin, E. N. Kislovskii, E. G. Len, and E. V. Pervak, phys. stat. sol. (b) **231**, 199 (2002).
[29] F. S. Ham, J. Phys. Chem. Solids **6**, 335 (1958).
[30] I. M. Lifshitz and V. V. Slyozov, Zh. Eksp. Teor. Fiz. **35**, 479 (1958). C. Wagner, Z. Elektrochem. **65**, 581 (1961).
[31] M. Koiwa, Philos. Mag. **30**, 877 (1974).
[32] J. R. Patel, K. A. Jackson, and H. Reiss, J. Appl. Phys. **48**, 5279 (1977).
[33] K. Wada and N. Inoue, J. Cryst. Growth **71**, 111 (1985).
[34] S. M. Hu, Appl. Phys. Lett. **48**, 115 (1986).
[35] K. Sueoka, N. Ikeda, T. Yamamoto, and S. Kobayashi, J. Appl. Phys. **74**, 5437 (1993).
[36] S. Senkader, J. Esfandyari, and G. Hobler, J. Appl. Phys. **78**, 6469 (1995).
[37] B. C. Larson and F. W. Young, Jr., J. Appl. Phys. **48**, 880 (1977).
[38] J. R. Schneider, R. Bouchard, H. A. Graf, and H. Nagasawa, Acta Crystallogr. A **48**, 804 (1992).
[39] J. R. Patel, J. Appl. Phys. **44**, 3903 (1973).
[40] S. P. Murarka, J. Appl. Phys. **48**, 5020 (1977).
[41] W. Patrick, E. Hearn, W. Westdorp, and A. Bohg, J. Appl. Phys. **50**, 7156 (1979).
[42] K. Wada, N. Inoue, and K. Kohra, J. Cryst. Growth **49**, 749 (1980).
[43] F. M. Livingston, S. Messoloras, R. C. Newman, B. C. Pike, R. J. Stewart, W. J. Binns, W. P. Brown, and J. G. Wilkes, J. Phys. C **17**, 6253 (1984).